Calibration uncertainty of assembled array hydrophones

Dr. Y Gao, Mr. P. Harvey, Mr. P. Cooper and Mr. P. Baker
Thales Australia
274 Victoria Road, Rydalmere NSW 2116, Australia
email: yujin.gao@thalesgroup.com.au

Abstract **- This paper presents a method to predict the uncertainty of a procedure for calibration of fully assembled array hydrophones in a shallow water environment. All error sources (due to measurement elements, instruments, background noise, calibration setup and environment) of the calibration procedure are defined and combine to predict the final calibration uncertainty theoretically. The methodology for predicting the calibration uncertainty is also validated using actual trial measurements in a shallow estuary.**

I. Introduction

Accurate calibration of a sonar sensor array is important if the data collected is to support reliable estimation of acoustic levels in the water and to improve the performance of array processing. While individual hydrophone elements are accurately characterized prior to assembly into complex array structures, the finished array sensitivity is influenced by the mechanical materials and construction techniques, and the performance of built-in amplifiers and digitization components

Ref. [1] reviewed various methods for calibrating underwater electroacoustic sensors in a reverberant tank, where free-field measurements (no contamination by echoes from the boundaries of the tank) are required for calibration purpose. In the case where echoes are involved, techniques, such as cross-correlation and cepstral deconvolution, are proposed to remove them. The calibration results presented in [1] are all above 1 kHz, which is specified as 'low frequency calibration'. For calibrating fully assembled array hydrophones, the frequency range to be calibrated could vary from several Hz to several thousand Hz, which makes it very difficult to use free-field measurements in a test tank.

In this paper a procedure to calibrate fully assembled array hydrophones is discussed, but with emphasis on analysis of its calibration uncertainty. This procedure is designed to be used in a shallow water environment due to the limitation of available deep water calibration sites (in a suitably protected environment) in Australia. In principle, the procedure can be used to calibrate assembled array hydrophones in any shape of array (e.g. a linear array or a cylindrical one).

In the calibration process, reference hydrophones and array hydrophones are positioned next to each other, as shown in Fig. 1. A transmitter, Tx, is used to produce a required calibration tone signal. This tone signal is simultaneously measured by the reference hydrophones and array

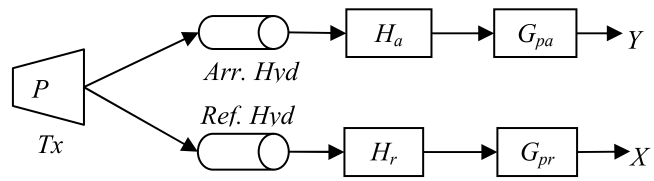

Figure 1. Block diagram of the calibration procedure.

hydrophones, amplified and converted to digital signals through the measurement chain. The digital signals are then passed through a signal processing chain to obtain their spectra.

The variables shown in Fig. 1 are functions of frequency and defined as follows:

- H_a - TF (Transfer Function) of array hydrophones to be calibrated ($U/\mu Pa$),
- H_r - TF of reference hydrophones, absolutely calibrated ($U/\mu Pa$),
- G_{Pa} - spectral gain of signal processing for array hydrophone,
- G_{Pr} - spectral gain of signal processing for reference hydrophone,
- P - acoustic pressure at Tx (μPa),
- Y - spectral amplitude of array hydrophone, and
- X - spectral amplitude of reference hydrophone.

In a shallow water environment significant surface and bottom reflections occur so multiple reference hydrophones are carefully positioned to spatially sample the sound field variability over the extent of array hydrophones to be calibrated. This provides the flexibility to use more than one reference hydrophone to calibrate a single array hydrophone, which is particularly useful in the case where an array hydrophone can not be positioned next to a reference hydrophone due to various practical limitations.

By setting the spectral gains in the signal processing to unity (with proper normalization) in Fig. 1, the calibrated TF, H_a, of the array hydrophones can be expressed using the spectral amplitudes, X and Y,

$$H_a = \frac{Y}{X} H_r , \quad (1)$$

which is the same as (3.5) in [1] and used to calculate the calibrated TF in the procedure here.

The calibration uncertainty is the error in H_a resulting from the combination of all the errors in the measurement chain and signal processing in the procedure (Fig. 1). These errors will

978-1-4244-5222-4/10/$26.00 ©2010 CROWN

be defined in Section II. In Section III we derive the theoretical calibration uncertainty for the procedure. In Section IV, the calibration uncertainty derived theoretically is compared against an actual trial measurement made in a shallow estuary.

II. ERROR SOURCES

In the derivation of (1), we have made two assumptions. The first is that the reference hydrophone is sampling the same sound pressure level as at the array hydrophone. In fact a reference hydrophone and an array hydrophone can not be exactly coincident in the sound field and a deviation of sound pressure measured by the two hydrophones always exists. The second is that the signal processing gains for both reference and array hydrophones are properly normalized to unity, which can be implemented very easily in practice. However, the hardware in the reference hydrophone chain can be different from that in the array hydrophone chain. For system hardware reasons we are unable to measure the reference and array hydrophone signals with the same sampling clock. In such a case different signal processing operations are needed. Each signal processing operation could result in a small fluctuation of the signal processing gains (see later).

For analysis of calibration uncertainty, we have to include all the links (measurement set up, hardware, software and environment) in the calibration chain, which result in various error sources. These links are shown in Fig. 2 and some of them can be further divided in to sub-links (see later).

From Fig. 2, the spectral amplitudes, Y and X, at the output are,

$$Y = P_a \cdot H_a \cdot G_{Pa}\,, \tag{2}$$

and

$$X = P_r \cdot S_r \cdot G_c \cdot G_s \cdot G_{\mathrm{Pr}}\,. \tag{3}$$

where,

- G_c - gain of conditioning amplifier,
- G_s - gain of sound card,
- P_a - acoustic pressure at the array hydrophone (μPa),
- P_r - pressure at the reference hydrophone (μPa),
- S_r - sensitivity of the reference hydrophone ($v/\mu Pa$).

From (2) and (3) the TF of an array hydrophone can be written as,

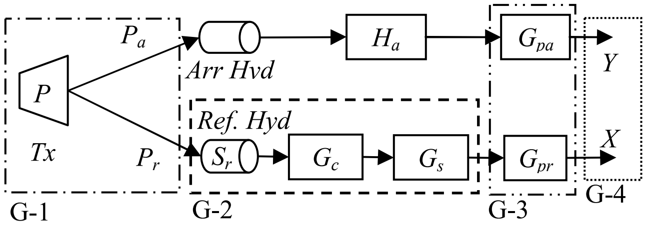

Figure 2. Calibration chain showing links resulting in various error sources.

$$H_a = \frac{P_r}{P_a} \cdot S_r \cdot G_c \cdot G_s \cdot \frac{G_{\mathrm{Pr}}}{G_{Pa}} \cdot \frac{Y}{X}\,. \tag{4}$$

All the variables in the RHS of (4) affect the calibrated TF and their errors contribute to the uncertainty of the calibrated TF. For convenience, these errors can be analyzed in four groups.

The first group of errors (G-1) is due to the measurement set-up (the dash-dot-line rectangle in Fig. 2). With the set-up of transmitter, array and reference hydrophones as discussed above, the pressure P_a at an array hydrophone and the pressure P_r at a reference hydrophone can differ according to the transmitter (Tx) directivity, the propagation path length variations and multipath interferences (see later).

The second group of errors (G-2) is contributed by the hardware in the reference hydrophone branch, as marked by the dashed-line rectangle in Fig. 2. They are the errors of reference-hydrophone sensitivity (S_r), conditioning amplifier gain (G_c) and sound card gain (G_s). Note that the transfer function, H_a, in the array hydrophone branch includes the contribution of all the assembled array hardware from the pressure input to the digital samples at the output (including preamp and ADC) and is the quantity to be calibrated.

The third group of errors (G-3) is associated with the signal processing applied to both the array and reference hydrophone signals (the dash-dot-dot line rectangle in Fig. 2), and are mainly due to the filtering operation and scalloping loss (see later) after neglecting the error of digital rounding.

The last group of errors (G-4) is caused by using the spectral amplitudes, Y and X, at the SP output to derive the transfer function in (1) without considering the noise contamination in the calibration process (the square-dot-line rectangle in Fig. 2).

III. CALIBRATION UNCERTAINTY

For error analysis of the calibration procedure, each variable in (4) is modeled as its mean value plus a random variable, i.e.,

$$Z = \overline{Z} + \Delta Z = \overline{Z}\,(1 + z)\,, \tag{5}$$

where,

$$z = \Delta Z / \overline{Z}\,. \tag{6}$$

The specification of the calibration uncertainty is usually defined as a dB quantity. As shown in Appendix A the uncertainty (in dB) of Z is only related to the normalized variable z, also called the relative error. We will derive the SD (Standard Deviation) of the relative error, z, related to each individual variable, which results in an error in the calibrated TF, and express the calibration uncertainty as a function of all the derived SDs in the following discussion. In all the derivations we assume $|z| << 1$.

A. *Errors due to Measurement Set-up*

Fig. 3 shows the block diagram for analyzing the errors due to measurement set-up. All the variables in the middle blocks are modeled as a gain (or loss).

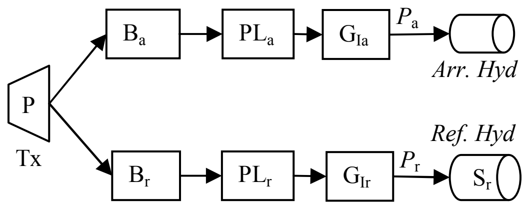

Figure 3. Block diagram for analysing the errors due to measurement set-up.

Here:

- Ba - amplitude of Tx directivity pointing at the array hydrophone,
- Br - amplitude of Tx directivity pointing at the reference hydrophone,
- GIa - gain of multipath interference at the array hydrophone,
- GIr - gain of multipath interference at the reference hydrophones,
- PLa - propagation loss from the transmitter to the array hydrophone, and
- PLr - propagation loss from the transmitter to the reference hydrophone.

The pressure, P_a and P_r, in the frequency domain can be written as,

$$P_a = P \cdot B_a \cdot PL_a \cdot G_{Ia} \ , \tag{7}$$

and,

$$P_r = P \cdot B_r \cdot PL_r \cdot G_{Ir} \ . \tag{8}$$

From (7) and (8) we obtain,

$$\frac{P_r}{P_a} = \frac{B_r}{B_a} \cdot \frac{PL_r}{PL_a} \cdot \frac{G_{Ir}}{G_{Ia}} \ . \tag{9}$$

A.1. Error in Tx directivity

The directivity of the transmitter will have an impact on the measurement. For an omni-directional transmitter with a piston, its directivity variation is much smaller in a thin annular ring around the piston axis than in any other thin annular ring perpendicular to the former. This feature is used in setting up the calibration measurements by positioning both array and reference hydrophones in a limited height zone when the transmitter is mounted with a vertical piston axis. In this way we only need to consider the directivity variations within the spherical angles, which cover the space of the hydrophones in the measurement.

The transmitter is omni-directional and has a nominal gain of unity with a small fluctuation. The respective amplitudes of the directivity pointing at an array hydrophone and a reference one are,

$$B_a = 1 + b_a \tag{10}$$

and,

$$B_r = 1 + b_r \ . \tag{11}$$

The directivity variation is treated as a Gaussian distribution. Both b_a and b_r are bounded by $\pm b_{max}$ and we use this as an estimate of the 3 sigma bound around its mean. Thus the SDs of b_a and b_r are,

$$\sigma_{ba} = \sigma_{br} = b_{\max} / 3 \ . \tag{12}$$

From (9) and (12), the variance due to the variation of the Tx directivity can be derived as,

$$\sigma^2_{BP} = Var\ \left[(1 + b_r)/(1 + b_a)\right] \approx \sigma^2_{ba} + \sigma^2_{br} \ . \tag{13}$$

A.2. Error in Propagation Path Length

Assuming that the source signal is spherically spreading, the propagation losses from the Tx to an array hydrophone and to a reference one are,

$$PL_a = 1/R_a \ , \tag{14}$$

and

$$PL_r = 1/R_r \ . \tag{15}$$

R_a and R_r are the respective propagation path lengths.

The Tx is flexibly supported to isolate the vibration of the test equipment and its position can potentially move within a sphere of r m radius. The Tx movement is assumed to be a Gaussian variable considering the nature of the oscillation of the test equipment in water and the SD of the movement is,

$$\sigma_{Tx} = r \ /3 \ . \tag{16}$$

The range errors between Tx and a hydrophone is bounded by ΔR, which is treated as a three sigma estimate, i.e.,

$$\sigma_{\Delta R} = \Delta R/3 \ . \tag{17}$$

This error is caused by the test equipment and hydrophone mounting.

Let the respective range errors to an array hydrophone and a reference hydrophone be r_a and r_r, which are caused by the random movement of the TX, and let the respective range errors related to hydrophone mounting be ΔR_a and ΔR_r, the actual propagation path length to an array hydrophone is,

$$R_a = \overline{R}_a \left(1 + (r_a + \Delta R_a)/\overline{R}_a\right). \tag{18}$$

and that to a reference hydrophone is,

$$R_r = \overline{R}_r \left(1 + (r_r + \Delta R_r)/\overline{R}_r\right). \tag{19}$$

From (9), (14), (15), (18) and (19) we can obtain the SD caused by the variation of propagation path length,

$$\begin{aligned} \sigma^2_{PL} &= Var\left[\left(1 + (r_a + \Delta R_a)/\overline{R}_a\right)/\left(1 + (r_r + \Delta R_r)/\overline{R}_r\right)\right] \\ &\approx \left(\sigma^2_{Tx} + \sigma^2_{\Delta R}\right)\left(\overline{R}_a^{-2} + \overline{R}_r^{-2}\right) \end{aligned} \tag{20}$$

A.3. Multipath Interference

Fig. 4 shows the multipath propagation and the relative positions between a hydrophone and the transmitter (Tx). The Tx is located in a shallow water medium Z_s m deep from the surface and Z_b m above the bottom. B is the horizontal distance between the Tx and the hydrophone. The hydrophone is z m above the Tx.

The direct path length from the Tx to the hydrophone is,

$$R_{dz} = \sqrt{B^2 + z^2} \ . \tag{21}$$

The surface path length is,

$$R_{sz} = \sqrt{B^2 + (2Z_s - z)^2} \ . \tag{22}$$

The bottom path length is,

$$R_{bz} = \sqrt{B^2 + (2Z_b + z)^2} \ . \tag{23}$$

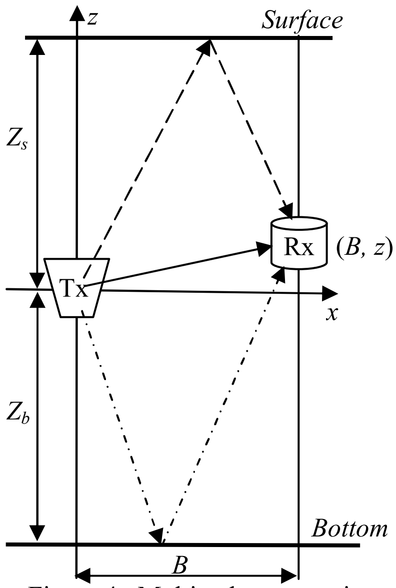

Figure 4. Multipath propagation

For the transmitted CW source at Tx,

$$p(t) = Ae^{j\omega t} , \tag{24}$$

the pressure measured at Rx can be expressed as,

$$p(t,z) = \frac{A}{R_{dz}} e^{j(\omega t - kR_d)} + \frac{\alpha_s A}{R_{sz}} e^{j(\omega t - kR_s)} + \frac{\alpha_b A}{R_{bz}} e^{j(\omega t - kR_b)} , \tag{25}$$

where,

α_s coefficient of surface reflection, and

α_b coefficient of bottom reflection.

The multipath interference gain in (9) is defined as the absolute ratio of the pressure measured at the hydrophone and that of the direct propagation. Let $a_z = \alpha_s R_{dz}/R_{sz}$ and $b_z = \alpha_d R_{dz}/R_{bz}$, the interference gain can be written as,

$$G_I(f,z) = \left|1 + a_z e^{jk(R_{dz} - R_{sz})} + b_z e^{jk(R_{dz} - R_{bz})}\right| , \tag{26}$$

where, k is the wave number and,

$$k = 2\pi f / c . \tag{27}$$

Eq. (26) can be applied to either an array hydrophone or a reference one, both $a_z << 1$ and $b_z << 1$ and the ratio of the two gains is,

$$G_{Ir} / G_{Ia} \approx 1 + g . \tag{28}$$

The error resulting from the multipath interference is,

$$\begin{aligned} g = 0.5[& a_{zr}^2 + b_{zr}^2 + 2a_{zr}\cos k(R_{szr} - R_{dzr}) \\ & + 2b_{zr}\cos k(R_{bzr} - R_{dzr}) - 2a_{zr}b_{zr}\cos k(R_{szr} - R_{bzr}) \\ & - a_{za}^2 - b_{za}^2 - 2a_{za}\cos k(R_{sza} - R_{dza}) \\ & - 2b_{za}\cos k(R_{bza} - R_{dza}) + 2a_{za}b_{za}\cos k(R_{sza} - R_{bza})] \end{aligned} . \tag{29}$$

When an array hydrophone is coincident with reference one ($z_a = z_r$) the multipath interference error becomes zero (g = 0).

In (29) g is a function of reflection coefficients (surface and bottom), Tx positions and those of array and reference hydrophones and water depth. In practice the Tx position is affected by surface waves and the motion of test equipment in the water column. The water depth is also affected by surface waves even at a selected test site. Also g is the sum of 10 variables (or functions of random variables). Considering the above conditions and Central Limit Theorem [2] g is assumed to be Gaussian.

In order to estimate the error due to multipath interference in (29), a numerical calculation is required for a selected test environment, from which the water depth, the transmitter depth and the bottom reflection coefficient can be measured. In the current investigation the interference errors are calculated over the whole frequency band and over the spatial volume covering all the array hydrophones, which are calibrated using the same reference sound level. The numerically calculated maximum error, g_{max}, is used as the 3 sigma estimate of the multipath interference error, i.e.,

$$\sigma_g = g_{\max} / 3 . \tag{30}$$

The above estimation is conservative because the maximum error occurs in the high frequency region and at a hydrophone furthest away from the reference one (see later).

All the errors due to the measurement set up are independent and small. The SD of the first Group of errors (G-1) is (see Appendix B),

$$\sigma_{G1} = \sqrt{\sigma_{BP}^2 + \sigma_{PL}^2 + \sigma_g^2} . \tag{31}$$

B. Errors in the hardware of reference hydrophones

There are three elements in the hardware of reference hydrophones as shown in Fig. 2, namely reference hydrophone, conditioning amplifier and sound card. The hardware uncertainties could change with time. A regular calibration of them is required and can be implemented either by a standards and test laboratory or through an in-house calibration procedure. Here the product uncertainty specifications of the three hardware elements are used. Usually these uncertainties are the two sigma error bounds and have a confidence level of 95%.

The reference hydrophones are of B & K type 8106. Its sensitivity uncertainty within the frequency band considered in the current investigation is 0.25 dB at 22.1C^o and the sensitivity changes with temperature at 0 - 0.01dB/C^o [4]. The sensitivity change with temperature is assumed to be independent of sensitivity errors and the temperature variation is assumed to be ±10 C^o. Based on the above assumption and the SD of the reference hydrophone sensitivity error is,

$$\sigma_r = \sqrt{0.25^2/2^2 + 0.1^2/3^2} / 8.69 = 0.0188. \tag{32}$$

The conditioning amplifier is of B & K Type 2690 [5] and its error uncertainty is 0.2 dB. The SD of the error due to the amplifier is,

$$\sigma_{ca} = 0.2/(2 \times 8.69) = 0.0115. \tag{33}$$

In the sound card, two errors are considered [6], one is frequency response variation and the other is quantization error.

The uncertainty of its frequency response is 0.25 dB [6] and the SD of this error is,

$$\sigma_{sc} = 0.25/(2 \times 8.69) = 0.0144. \tag{34}$$

The ADC in the sound card is a 24-bit digitizer. Quantization errors are of uniform distribution [7] and the SD of the quantization error after normalization is,

$$\sigma_{AD} = 1/\left(2^{24} \times \sqrt{3}\right) = 3.4 \times 10^{-8}, \qquad (35)$$

which can be neglected.

The errors generated by the three different hardware elements are independent and small. The SD of the second group of errors (G-2) is,

$$\sigma_{G2} = \sqrt{\sigma_r^2 + \sigma_{ca}^2 + \sigma_{sc}^2} = 0.0263. \qquad (36)$$

C. *Errors in signal processing*

The flow chart of signal processing is shown in Fig. 5. This is the core processing of the calibration calculation, which describes how the calibrated TFs of array hydrophones are derived using acoustic data measured by reference hydrophones and array hydrophones.

The processing flow for the reference hydrophone is almost identical to that of the array hydrophone. The only difference is the LP filtering and decimation at the beginning in order to re-sample reference hydrophone signals in a required rate. From the signal processing chain, three mechanisms of error generation can be identified. The first one is the LP filtering applied to reference hydrophone signals. The second is caused by the windowing and FFT operations. These two mechanisms will be addressed in this section.

The last mechanism is associated with the noise contamination in the estimate of the tone spectral magnitudes. Strictly speaking it is not due to signal processing, but stems from background acoustic noise at the hydrophones in the water and will be addressed in a subsequent section.

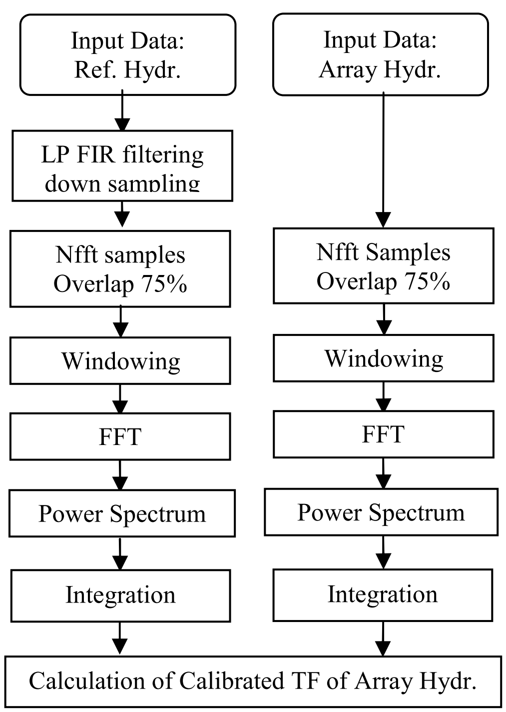

Figure 5. Flow chart of signal processing.

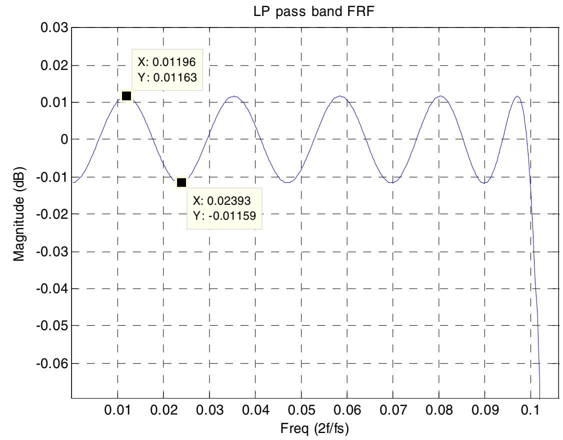

Fig. 6. LP filter pass band response

The LP filter is of Parks-McClellan equiripple. It minimizes the filter length for a given filter specification, while allowing the passband ripple to be minimised. The frequency response of the LP filter is shown in Fig. 6, which shows a ripple of ±0.012dB in the passband. The ripple has a sinusoidal form and its SD is,

$$\sigma_{LP} = 0.012 / \left(8.69 \times \sqrt{2}\right) = 0.0010 \ . \qquad (37)$$

The errors related to the windowing and FFT operations are caused by the so-called scalloping loss [8] and different sampling clock rates between the array and reference hydrophones. In the case where the sampling rates for the array and reference hydrophones are the exactly same these errors are mutually cancelled because the ratio between the array and reference hydrophone spectra is used in (4). In the calibration procedure, two different sampling clocks are used and the sampling clock error in reference hydrophones is 0.000079 sec and that in array hydrophones is 0.000008 sec. This produces a significant frequency difference at the high frequency region.

In order to reduce the error discussed above the so-called flat-top window is used in signal processing [8]. Fig. 7 shows that the maximum scalloping loss is 0.016 dB and occurs at the extremity of the bin (one half bin-widths from the centre of the bin). The value of the difference can be

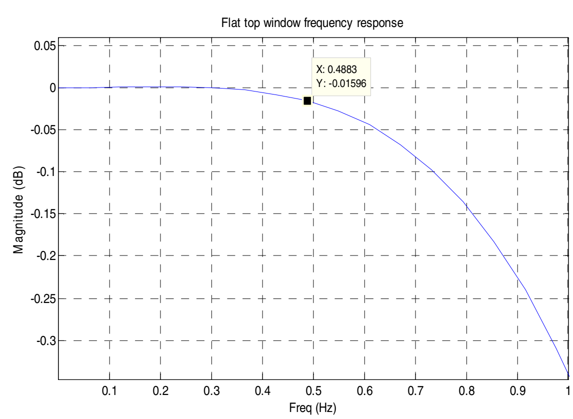

Figure 7. Response of flat top window

positive or negative depending on alignment of frequencies with bins, and is assumed to be Gaussian distribution (over the range ±0.016 dB). The SD is therefore calculated by,

$$\sigma_w = 0.16/(3\times 8.69) = 0.0006 \ . \quad (38)$$

By combining (37) and (38) we obtain the SD of the third group of errors (G-3),

$$\sigma_{G3} = \sqrt{\sigma_{LP}^2 + \sigma_w^2} = 0.0012. \quad (39)$$

D. Errors due to background acoustic noise

The signals measured by both array and reference hydrophones contain random background acoustic noise, N_a and N_r, as shown in Fig. 8. H_a and H_r are the respective TFs of array and reference hydrophones from the acoustic level in the water to the SP output.

The integrated power spectra at the output are of non-central Chi-squared distribution. Assuming that the background noise has a zero mean and a SD of σ, the CW signal has an amplitude of A and the number of spectrum integration is M, the mean and variance of the integrated power spectra (after normalized by their respective TFs) are,

$$\begin{aligned} m_{M\lambda} &= E[X^2]/H_r^2 = E[Y^2]/H_a^2 \\ &= \beta M\sigma^2 + MA^2/4 \end{aligned} , \quad (40)$$

and,

$$\begin{aligned} \sigma_{M\lambda}^2 &= \mathrm{var}[X^2]/H_r^4 = \mathrm{var}[Y^2]/H_a^4 \\ &= \beta^2 M\sigma^4 + \beta M\sigma^2 A^2/2 \end{aligned} , \quad (41)$$

where,

$$\beta = \sum w_k^2 \ , \quad (42)$$

and w_k is the coefficient of the flat top window and normalized such that its DC component is unity.

SNR is defined as the mean of the integrated power spectrum subtracted by the mean of the noise power spectrum and divided by the SD of the noise power spectrum. From (40) and (41) we have,

$$SNR = A^2\sqrt{M}/(4\beta\sigma^2). \quad (43)$$

In the derivation of (43) the consecutive power spectra are assumed to be uncorrelated. This needs to be discussed further in the case where overlapping is involved in the consecutive FFT operations. In the case of a flat top window, its ENBW is 3.77 [8] and the equivalent length of the FFT is approximately ¼ of the actual FFT length. This means that with a 75% overlap (Fig. 5) we can make the above assumption without introducing any considerable errors. In fact the error introduced by the assumption is related to the ratio between the number of spectrum integrations and the number of independent spectrum integrations [8]. It can be shown that this ratio error is less than 0.5% when a flat top window with an overlap of 75% is used.

The integrated power spectra at the output of signal processing can be expressed as their expected mean plus a small random variation, i.e.,

$$Y^2 = m_{M\lambda} H_a^2 (1+y), \quad (44)$$

and

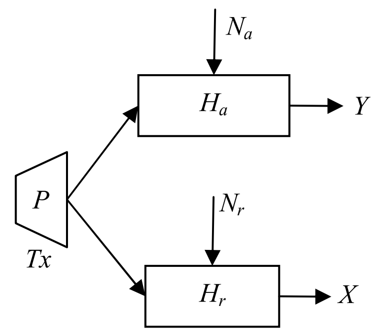

Figure 8. Errors due to background acoustic noise

$$X^2 = m_{M\lambda} H_r^2 (1+x), \quad (45)$$

where,

$$y = Y^2/(m_{M\lambda}H_a^2) - 1, \quad (46)$$

$$x = X^2/(m_{M\lambda}H_r^2) - 1, \quad (47)$$

and $|x| \ll 1$ and $|y| \ll 1$ and they are the normalized random variables. From (40 ~ 47) we can derive,

$$E[x] = E[y] = 0, \quad (48)$$

and,

$$\sigma_y^2 = \sigma_x^2 = \frac{1}{SNR}\frac{2/\sqrt{M} + 1/SNR}{\left(1+\sqrt{M}/SNR\right)^2} . \quad (49)$$

The amplitude ratio between the array and reference hydrophone spectra (after spectral integration) is,

$$\frac{Y}{X} = \frac{H_a}{H_r}\cdot\frac{\sqrt{1+y}}{\sqrt{1+x}} . \quad (50)$$

The SD of the relative error in (50) is,

$$\sigma_N = \sqrt{\mathrm{var}[\sqrt{1+y}/\sqrt{1+x}]} \approx \sigma_y\sqrt{(1-\gamma)/2} \quad (51)$$

which is also the SD of the fourth group of errors, i.e., σ_{G4}=σ_N, where,

$$\gamma = E[x\cdot y]/\sigma_y^2 \quad (52)$$

Eq. (51) shows that any correlation between the reference and array hydrophone signals will reduce the calibration error variance because of their mutual cancellation in the signal processing procedure. In the case where the array and reference hydrophones are located at the same position γ = 1 and background noise has no contribution to the calibration uncertainty.

Eqs (49) and (51) also show that the variance caused by background acoustic noise is a function of SNR and the number of spectral integrations.

Fig. 9 shows the relation between SDs and SNRs (after integration) for six different integration times when $\gamma = 0$ in (51). It can be seen that increasing integration time can reduce the variance. However, this reduction diminishes with SNR.

E. Uncertainty of the calibration procedure

By combining the four groups of errors discussed above the SD of the array hydrophone TF calibration errors is,

$$\sigma_{TF} = \sqrt{\sigma_{G1}^2 + \sigma_{G2}^2 + \sigma_{G3}^2 + \sigma_{G4}^2} \ . \quad (53)$$

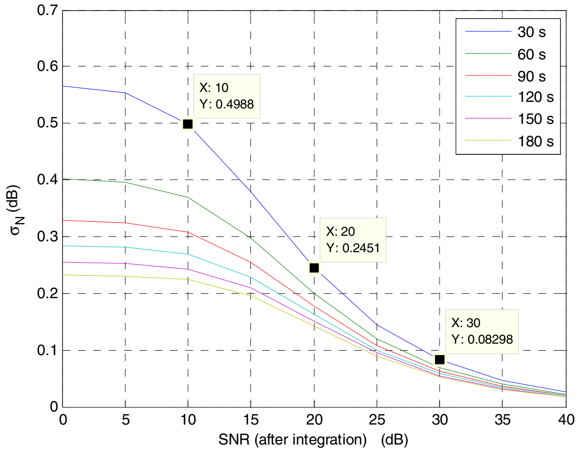

Figure 9. SD of uncorrelated acoustic noise in the water

IV. AN EXAMPLE

The error analysis technique discussed in this paper was used to predict the calibration uncertainty (or SD) of fully assembled array hydrophones. The calibration was carried out in a shallow estuary.

The Tx directivity error is bounded by 0.25dB and the error SD in (12) is,

$$\sigma_{BP} = 0.0136 \quad . \tag{54}$$

Both the Tx movement and range error between the Tx and hydrophones have a bound of 0.02m. The minimum propagation path length (1.53 m) is used to calculate the SD in (20). This leads to a conservative SD estimate, i.e.,

$$\sigma_{PL} \leq 0.0087 \quad . \tag{55}$$

The above error SD is caused by the range errors discussed above and the propagation loss related to the nominal path length has been compensated in the TF calibration.

The water depth is 21 m and the Tx is 15 m deep. The surface reflection coefficient is -1 and the bottom reflection coefficient is 0.56 (actually measured values). The hydrophones are positioned around the TX height (±0.35m). Fig. 10 shows the errors of multipath interference calculated using (29). The maximum error is 1.89 dB, leading to,

$$\sigma_g = 0.0725 \quad . \tag{56}$$

The SD of the first group of errors in (31) is

$$\sigma_{G1} = 0.0743 \quad . \tag{57}$$

In the calibration, the SNRs after spectrum integration are larger than 30 dB and the integration time is 30s. From Fig. 9, the SD for the fourth group of errors is 0.083dB, i.e.,

$$\sigma_{G4} = 0.0095 \; . \tag{58}$$

From (57), (36), (39) and (58) we obtain the SD of array hydrophone TF calibration erros in (53),

$$\sigma_{TF} = 0.0794 = 0.69\text{dB}. \tag{59}$$

Fig. 11 shows the normalized calibration errors resulting from 80 different calibration frequencies for 25 fully assembled array hydrophones. The SD of the calibration

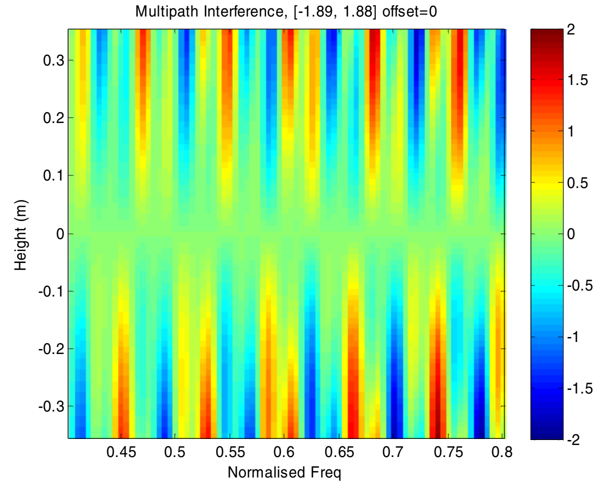

Figure 10. Multipath interference errors

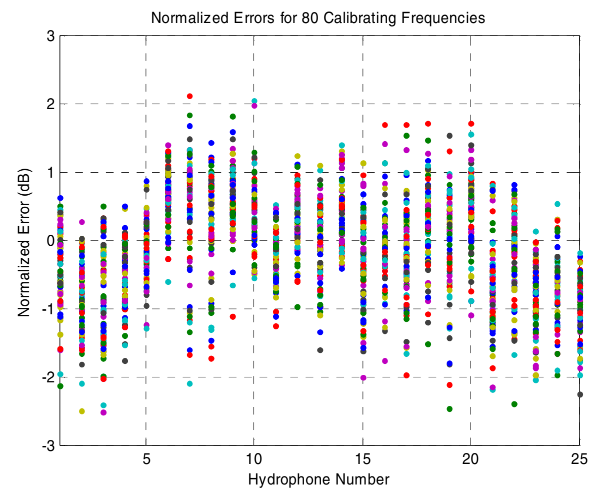

Figure 11. Normalized calibration errors resulted from 80 different calibrating frequencies for 25 fully assembled array hydrophones.

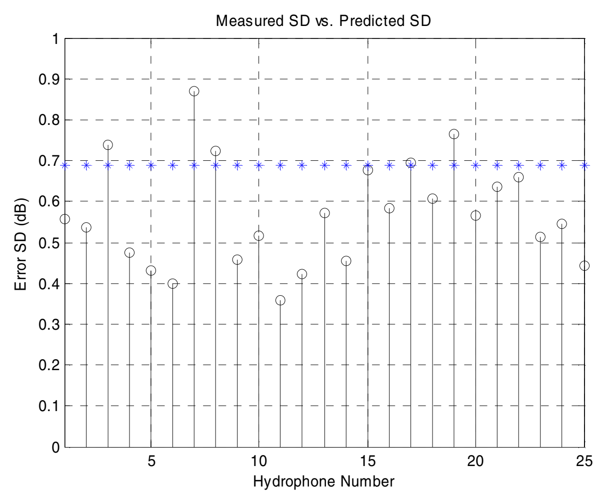

Figure 12. Comparison between the measured and predicted SDs of calibration errors.

errors for each individual hydrophone is shown in Fig. 12, where the stars represent the theoretically predicted SD of calibration errors. A very good agreement between the measured and predicted SD is achieved.

V. Conclusions

In this paper we presented a method for theoretically predicting the uncertainty of array hydrophone TF calibration. The development of the method is based on a calibration procedure which is used to calibrate fully assembled array hydrophones in a shallow water environment in Australia. The errors resulting in the uncertainty can be divided into four groups, namely, errors due to measurement set up, hardware, signal processing and background acoustic noise. These errors are thoroughly analyzed and it is demonstrated theoretically that the error variance of a hydrophone TF calibration is the sum of the error variances of the four groups. The calibration errors measured in a shallow estuary are also presented for 25 array hydrophones, each of which was calibrated at 80 different frequencies. The SDs calculated using the measured errors agree well with what is predicted theoretically.

Acknowledgment

Thales Australia Research and Technology Director Michael Clark provided valuable comments during the preparation of this paper. Y. G. appreciates the feedbacks from Dr. Didier Billon, Thales Under Water Systems S.A.S France.

References

[1] S. P. Robinson, "Review of methods for low frequency transducer calibration in reverberant tanks," *NPL report CMAM 034*, June 1999.

[2] A. Papoulis, *Probability, Random Variables, and Stochastic Process*, McGraw-Hill, Inc, 3rd Ed., 1991.

[3] L. Kirkup, *Experimental Methods*, John Wiley & Sons, Brisbane, 1994.

[4] B & K, *Calibration chart for hydrophone type 8106*.

[5] B & K, *Conditioning amplifier, B&K type 2690*.

[6] Audio Science, *multistream linear audioadapters*, WWW.audioscience.com.

[7] A. V. Oppenheim and R. W. Schafer, *Discrete Time Signal Processing*, Prentice-Hall, Inc. Englewood Cliff, NJ 07632, 1989.

[8] F. J. Harris, "On the use of windows for harmonic analysis with the discrete Fourier transform," *Proceedings of the IEEE*, Vol 66, No 1, Jan 1973.

Appendix A. Relation between dB variance and relative errors

For error analysis each quantity is modeled as its mean value plus a random fluctuation, i.e.,

$$Z = \overline{Z} + \Delta Z = \overline{Z}(1+z)\,, \tag{60}$$

where,

$$z = \Delta Z / \overline{Z}\,. \tag{61}$$

The dB-variance of Z is defined as,

$$\begin{aligned}\sigma_{zdB}^2 &= Var\left[20\log_{10}(Z)\right]\\ &= Var\left[20\log_e(1+z)/\log_e(10)\right]\end{aligned}. \tag{62}$$

When |z| << 1,

$$\sigma_{zdB}^2 \approx \left(20/\log_e(10)\right)^2 \operatorname{var}[z] = 8.6859^2\sigma_{zlin}^2\,. \tag{63}$$

In the above equation the variance (in dB) of Z is only related to the normalized variable z (relative error) and a linear conversion between the dB-SD and the linear-relative SD of the normalized variable z can be made,

$$\sigma_{zdB} \approx 8.69\sigma_{zlin}\,. \tag{64}$$

Appendix B. Error analysis

By combining Eqs (4) and (9), the calibrated TF of array hydrophones can be expressed in a general form,

$$TF = \prod_{i=1}^{I} Z_{ni} \Big/ \prod_{j=1}^{J} Z_{dj}\,. \tag{65}$$

Each individual factor in the above equation can be modeled as its own nominal mean plus a small random variation as in (60). Inserting (60) into (65) and assuming that all the normalized variables are much smaller than unity, we have,

$$TF \approx \left[\prod_{i=1}^{I} \overline{Z}_{ni} \Big/ \prod_{j=1}^{J} \overline{Z}_{dj}\right]\left(1 + \sum_{i=1}^{I} z_{ni} - \sum_{j=1}^{J} z_{dj}\right). \tag{66}$$

In the case where the normalized variables (z_{ni} and z_{dj}) are independent the variance of the normalized quantity is

$$\sigma_{TF}^2 \approx Var\left[1 + \sum_{i=1}^{I} z_{ni} - \sum_{j=1}^{J} z_{dj}\right] = \sum_{i=1}^{I}\sigma_{ni}^2 + \sum_{j=1}^{J}\sigma_{dj}^2\,. \tag{67}$$

In [3], a partial differential equation was used to derive the uncertainty of a quantity which is a function of multiple variables. All the variables contain random fluctuations, which contribute to the uncertainty. It can be shown that the same result can be achieved by using the partial differential equation in [3] as in (67).